

A FOURTH-ORDER UNFITTED CHARACTERISTIC FINITE ELEMENT METHOD FOR SOLVING THE ADVECTION-DIFFUSION EQUATION ON TIME-VARYING DOMAINS

CHUWEN MA*, QINGHAI ZHANG[†], AND WEIYING ZHENG[‡]

Abstract. We propose a fourth-order unfitted characteristic finite element method to solve the advection-diffusion equation on time-varying domains. Based on a characteristic-Galerkin formulation, our method combines the cubic MARS method for interface tracking, the fourth-order backward differentiation formula for temporal integration, and an unfitted finite element method for spatial discretization. Our convergence analysis includes errors of discretely representing the moving boundary, tracing boundary markers, and the spatial discretization and the temporal integration of the governing equation. Numerical experiments are performed on a rotating domain and a severely deformed domain to verify our theoretical results and to demonstrate the optimal convergence of the proposed method.

Key words. Unfitted characteristic finite element methods, time-varying domains, moving boundary problems, the advection-diffusion equation, fourth-order error estimates.

AMS subject classifications. 65M60, 65L06, 76R99

1. Introduction. Multiphase flows are ubiquitous in science and engineering and the study of them is of great significance in a wide range of applications. One core difficulty to numerical simulation is that the domain of each fluid phase may vary in time. In addition, the potentially large deformations of the domain boundary may incur complex interactions of multiple scales both in time and in space. When the thickness of the interface that separates the fluid from other phases is negligible, the tracking of the time-varying domain can be reduced to that of its boundary; in this case the problem is also referred to as a moving boundary problem.

The fidelity of numerically simulating physical processes on a time-varying domain is very much influenced by the locus of the moving boundary within each time step. On the one hand, interface tracking incurs errors that will inevitably affect the accuracy of the entire numerical simulation. On the other hand, sometimes the velocity field needed for interface tracking is not known a priori but can only be deduced from the state of the bulk fluid; this is especially true for realistic multiphase flows such as air-water free-surface flows. This potentially tight coupling of the fluid and the interface in moving boundary problems poses great challenges to computational scientists.

There are mainly two approaches in solving partial differential equations (PDEs) on domains with irregular and moving boundaries. In the body-fitted methods, the discretization mesh is *moved* at each time step to follow the time-varying domain so that constitutive laws as well as kinematic conditions on the deforming boundary can be imposed conveniently. Another popular category is

*⁽¹⁾ School of Mathematical Science, University of Chinese Academy of Sciences. ⁽²⁾ Institute of Computational Mathematics and Scientific/Engineering Computing, Academy of Mathematics and Systems Science, Chinese Academy of Sciences, Beijing, 100190, China. The first author was supported by National Key R & D Program of China 2019YFA0709600 and 2019YFA0709602. (chuwenii@lsec.cc.ac.cn)

[†]School of Mathematical Sciences, Zhejiang University, 38 Zheda Road, Hangzhou, Zhejiang Province, 310027 China. The second author was supported in part by China NSF grant 11871429. (qinghai@zju.edu.cn)

[‡]⁽¹⁾ LSEC, NCMS, Institute of Computational Mathematics and Scientific/Engineering Computing, Academy of Mathematics and Systems Science, Chinese Academy of Sciences, Beijing, 100190, China. ⁽²⁾ School of Mathematical Science, University of Chinese Academy of Sciences. The third author was supported in part by the National Science Fund for Distinguished Young Scholars 11725106, by China NSF grant 11831016, and by National Key R & D Program of China 2019YFA0709600 and 2019YFA0709602. (zwy@lsec.cc.ac.cn)

the unfitted methods, in which the underlying mesh, once generated, is *fixed* for all time steps and the moving interface is allowed to cut cells or elements of the static mesh. Despite its special treatment for cut elements, the unfitted methods are attractive in developing high-order schemes.

Unfitted methods have been highly successful. For stationary interface problems, popular unfitted methods include the immersed interface method (IIM) [15, 16], the immersed finite element method (IFEM) [17], the extended finite element method (XFEM) [4, 7], the cut finite element method [2], the interface-penalty finite element method [10, 25], the fictitious domain method [1, 11] and many others. For moving boundary problems, Fires and Zilian presented a first-order XFEM method by using the backward Euler method for time integration [6]. Based on a space-time discontinuous Galerkin discretization, Lehenfeld and Reusken [13] proposed a two-dimensional second-order XFEM scheme, which was extended to three dimensions by Lehenfeld in [12]. Recently, Guo [8] analyzed a backward Euler IFEM for solving parabolic moving interface problems. In [14], Lehenfeld and Olshanskii proposed an unfitted finite element method (UFEM) via utilizing the backward Euler method for time integration. More recently, Lou and Lehenfeld [19] extended the results in [14] by combining isoparametric UFEMs with k th-order backward differentiation formula (BDF- k) time stepping ($k = 1, 2, 3$); a priori error estimates are carried out for $k = 2$. In their work, the movements of curved boundaries are analytically prescribed and numerical errors arise only from the PDE discretization.

In spite of their successes, unfitted methods are not ready to be deployed in the study of realistic multiphase flows yet. One major roadblock is the lack of algorithmic coupling of main flow solvers to interface tracking methods. In current unfitted methods [5, 13, 19], it is usually assumed that explicit, analytic expressions have been given *a priori* to fully describe the movement of the boundary. However, this assumption does not hold for all realistic multiphase flows: more often than not the movement of the boundary must be determined *on the fly* from state variables of the main flow, e.g., the free-surface flows mentioned in the second paragraph. As the science of multiphase flows evolves towards more and more complex phenomena, there is a pressing need for coupling interface tracking algorithms to main flow solvers so that realistic moving boundary problems can be simulated accurately and efficiently.

We answer this need by developing a fourth-order unfitted characteristic finite element method (UCFEM) for numerically solving the advection-diffusion equation (2.1) on time-varying domains. Our method combines three main components: a fifth-order cubic MARS method [26] for interface tracking, a fourth-order BDF-4 scheme [18] for integrating a Lagrangian form of the advection-diffusion equation, and a UFEM with piecewise bi-quartic functions for spatial discretization. The computational domain is a fixed Eulerian mesh that covers the full movement range of the time-varying domain where the advection-diffusion equation holds.

The contributions of this work lie in three aspects.

- (a) Our method is the first fourth-order unfitted method for solving moving boundary problems via incorporating a fifth-order interface tracking method. This is not surprising since fourth- and higher-order interface-tracking algorithms have not been available until recently [26]. To the best of our knowledge, these algorithms have been coupled neither to finite element methods nor to finite difference/volume methods. Although we assume that the movement of the domain boundary is prescribed by analytic expressions, the interface tracking algorithm adopted in our method paves the way to future designs of more sophisticated methods that will be able to handle tight couplings of the fluid and the boundary.
- (b) We prove the stability of numerical solutions under the energy norm. In the Lagrangian frame, there is an essential difference between the proofs for second-order and fourth-order schemes.

In the latter case, numerical solutions from early time steps must serve as test functions at the present time step, while they do not belong to the present finite element space. We overcome this difficulty by defining a modified Ritz projection onto the finite element space.

- (c) Our convergence analysis includes error estimates not only for boundary representation and tracing boundary markers, but also for spatial discretization and temporal integration of the governing equation. As the main conclusion, the overall error is $O(\tau^4)$ under the energy norm for $h = O(\tau)$, where τ and h are the time-step size and the spatial mesh size, respectively.

The rest of the paper is organized as follows. In Section 2, we formulate the model problem using Lagrangian coordinates. In Section 3, we present the interface tracking algorithm and estimate the error between the exact boundary and the numerically approximated result. In Section 4, we propose the fourth-order UCFEM and prove the well-posedness of the discrete problem. In Section 5, we define the modified Ritz projection and prove the stability of numerical solutions. Section 6 is devoted to a priori error estimates of numerical solutions. In Section 7, we demonstrate the optimal convergence of our method by results of several numerical experiments.

Throughout this paper, $f \lesssim g$ means $f \leq Cg$ with a generic constant $C > 0$ independent of τ , h , and the segment size η for interface tracking; $f \approx g$ means that $f \lesssim g$ and $g \lesssim f$ hold simultaneously. Vector-valued quantities are denoted by boldface symbols, such as $\mathbf{L}^2(\Omega) = L^2(\Omega)^2$, and matrix-valued quantities are denoted by blackboard bold symbols, such as $\mathbb{L}^2(\Omega) = L^2(\Omega)^{2 \times 2}$.

2. The model problem. The advection-diffusion equation with initial and boundary conditions reads

$$\frac{\partial u}{\partial t} + \mathbf{w} \cdot \nabla u - \Delta u = f \quad \text{in } \Omega_t, \quad (2.1a)$$

$$u = 0 \quad \text{on } \Gamma_t, \quad (2.1b)$$

$$u(0) = u_0 \quad \text{in } \Omega_0, \quad (2.1c)$$

where $\Omega_t \subset \mathbb{R}^2$ is a bounded and simply-connected domain with time-varying boundary $\Gamma_t = \partial\Omega_t$, $\mathbf{w}(\mathbf{x}, t)$ is a given function satisfying $\text{div } \mathbf{w} = 0$, $u(\mathbf{x}, t)$ stands for the tracer transported by the fluid, and $f(\mathbf{x}, t)$ stands for the source term distributed in \mathbb{R}^2 and has a compact support. The equation has been scaled so that the diffusion coefficient before Δu is unit. We restrict the computations to a finite time interval $[0, T]$.

First, we make an assumption on the fluid velocity and the moving boundary.

ASSUMPTION 2.1. We assume that $\mathbf{w} \in \mathbf{C}^6(\mathbb{R}^2 \times [0, T])$ and has compact support, and that Γ_t is C^4 -smooth for all $t \in [0, T]$.

The physical domain is driven by the fluid velocity \mathbf{w} and is defined via the flow map

$$\Omega_t := \{\mathbf{X}(t; 0, \mathbf{x}) : \mathbf{x} \in \Omega_0\}, \quad (2.2)$$

where $\mathbf{X}(t; s, \cdot)$ is defined by the solution to the ordinary differential equations

$$\frac{d}{dt} \mathbf{X}(t; s, \mathbf{x}) = \mathbf{w}(\mathbf{X}(t; s, \mathbf{x}), t), \quad \forall t > s \geq 0; \quad \mathbf{X}(s; s, \mathbf{x}) = \mathbf{x}. \quad (2.3)$$

Since \mathbf{w} is \mathbf{C}^6 -smooth, (2.3) has a unique solution for every $s \in [0, T]$ and every $\mathbf{x} \in \mathbb{R}^2$. This implies that $\mathbf{X}(t; s, \cdot) : \Omega_s \rightarrow \Omega_t$ is a diffeomorphism.

For any $\mathbf{x}_0 \in \Omega_0$, we use the flow map \mathbf{X} to write $\mathbf{x} \equiv \mathbf{x}(t) = \mathbf{X}(t; 0, \mathbf{x}_0)$. The material derivative of u is defined as

$$\frac{d}{dt}u(\mathbf{x}(t), t) = \frac{\partial u}{\partial t}(\mathbf{x}, t) + \mathbf{w}(\mathbf{x}, t) \cdot \nabla_{\mathbf{x}}u(\mathbf{x}, t). \quad (2.4)$$

Then (2.1) can be written in an equivalent form

$$\frac{du}{dt} - \Delta u = f \quad \text{in } \Omega_t, \quad u = 0 \quad \text{on } \Gamma_t, \quad u(0) = u_0 \quad \text{in } \Omega_0. \quad (2.5)$$

3. The interface tracking algorithm. In this section, we explain the cubic MARS algorithm that we use to approximate the moving boundary. Then we establish rigorous error estimate for interface tracking.

Let $t_n = n\tau$, $n = 0, 1, \dots, N$, be a uniform partition of the interval $[0, T]$, where $\tau = T/N$ is the time step size. For convenience, we write $\mathbf{X}^{m,n} := \mathbf{X}(t_n; t_m, \cdot)$ for any $n \geq m > 0$ and use the shorthand notation $\mathbf{X}^{n,m} := (\mathbf{X}^{m,n})^{-1}$.

3.1. Discrete flow maps. Let $\mathbf{X}_\tau^{n-1,n}$ be the approximation of $\mathbf{X}^{n-1,n}$ such that $\mathbf{x}^n = \mathbf{X}_\tau^{n-1,n}(\mathbf{x}^{n-1})$ is defined by a fifth-order Runge-Kutta (RK-5) scheme (cf. [24]) for solving (2.3) from t_{n-1} to t_n . The multi-step discrete flow map is defined as $\mathbf{X}_\tau^{n-i,n} = \mathbf{X}_\tau^{n-1,n} \circ \mathbf{X}_\tau^{n-2,n-1} \circ \dots \circ \mathbf{X}_\tau^{n-i,n-i+1}$, $1 \leq i \leq n$. Similarly, the inverse of $\mathbf{X}_\tau^{n-i,n}$ is denoted by $\mathbf{X}_\tau^{n,n-i} := (\mathbf{X}_\tau^{n-i,n})^{-1}$.

For any $t \geq s \geq 0$ and $\mathbf{x} \in \mathbb{R}^2$, the Jacobi matrix of the flow map is defined as

$$\mathbb{J}(t; s, \mathbf{x}) := \nabla_{\mathbf{x}}\mathbf{X}(t; s, \mathbf{x}) = \mathbb{I} + \int_s^t \nabla_{\mathbf{x}}\mathbf{w}(\mathbf{X}(\xi; s, \mathbf{x}), \xi) \mathbb{J}(\xi; s, \mathbf{x}) d\xi. \quad (3.1)$$

Since $\text{div } \mathbf{w} = 0$, we have $\det(\mathbb{J}) \equiv 1$ for all $t \geq s$ (see e.g. [3]). Using Gronwall's inequality and Assumption 2.1, it is easy to show

$$\|\mathbb{J}(t; s, \cdot)\|_{\mathbb{W}^{5,\infty}(\mathbb{R}^2)} \lesssim 1, \quad \|\mathbb{J}(t_n; t_{n-i}, \cdot) - \mathbb{I}\|_{\mathbb{L}^\infty(\mathbb{R}^2)} \lesssim \tau, \quad 1 \leq i \leq 4. \quad (3.2)$$

Let the Jacobi matrices of $\mathbf{X}^{n-i,n}$ and $\mathbf{X}_\tau^{n-i,n}$ be denoted, respectively, by

$$\mathbb{J}^{n-i,n}(\mathbf{x}) := \mathbb{J}(t_n; t_{n-i}, \mathbf{x}), \quad \mathbb{J}_\tau^{n-i,n}(\mathbf{x}) := \nabla_{\mathbf{x}}\mathbf{X}_\tau^{n-i,n}(\mathbf{x}).$$

Similarly, the Jacobi matrices of $\mathbf{X}^{n,n-i}$ and $\mathbf{X}_\tau^{n,n-i}$ are denoted, respectively, by

$$\mathbb{J}^{n,n-i} := (\mathbb{J}^{n-i,n})^{-1}, \quad \mathbb{J}_\tau^{n,n-i} := (\mathbb{J}_\tau^{n-i,n})^{-1}.$$

Since $\mathbf{X}_\tau^{n-1,n}$ is obtained by the RK-5 scheme for (2.3), the one-step error is $O(\tau^6)$. For any bounded domain $D \subset \mathbb{R}^2$, standard error estimates give

$$\|\mathbf{X}_\tau^{n-1,n} - \mathbf{X}^{n-1,n}\|_{\mathbb{L}^\infty(D)} \lesssim \tau^6. \quad (3.3)$$

Moreover, taking the gradients of $\mathbf{X}^{n-1,n}$, $\mathbf{X}_\tau^{n-1,n}$ with respect to the spatial variable \mathbf{x} does not influence the order of temporal error estimates. So we also have

$$\|\mathbb{J}_\tau^{n-1,n} - \mathbb{J}^{n-1,n}\|_{\mathbb{L}^\infty(D)} \lesssim \tau^6. \quad (3.4)$$

Combining (3.2)–(3.4), we get

$$\|\mathbb{J}_\tau^{n-i,n} - \mathbb{I}\|_{\mathbb{L}^\infty(D)} \lesssim \tau, \quad \|\mathbb{J}_\tau^{m,n}\|_{\mathbb{W}^{5,\infty}(D)} \lesssim 1, \quad 1 \leq i \leq 4, \quad 0 \leq m < n. \quad (3.5)$$

Their inverses satisfy similar estimates

$$\|\mathbb{J}_\tau^{n,n-i} - \mathbb{I}\|_{\mathbb{L}^\infty(D)} + \|\mathbb{J}_\tau^{n,n-i} - \mathbb{I}\|_{\mathbb{L}^\infty(D)} \lesssim \tau, \quad \|\mathbb{J}_\tau^{n,m}\|_{\mathbb{L}^\infty(D)} + \|\mathbb{J}_\tau^{n,m}\|_{\mathbb{L}^\infty(D)} \lesssim 1. \quad (3.6)$$

Since $\mathbf{X}_\tau^{m,n} - \mathbf{X}^{m,n} = \sum_{j=m}^{n-1} (\mathbf{X}_\tau^{j+1,n} \circ \mathbf{X}_\tau^{j,j+1} - \mathbf{X}_\tau^{j+1,n} \circ \mathbf{X}^{j,j+1}) \circ \mathbf{X}^{m,j}$, the error estimates for multi-step maps can be obtained similarly

$$\|\mathbf{X}_\tau^{m,n} - \mathbf{X}^{m,n}\|_{\mathbf{W}^{\mu,\infty}(D)} + \|\mathbf{X}_\tau^{n,m} - \mathbf{X}^{n,m}\|_{\mathbf{W}^{\mu,\infty}(D)} \leq C(n-m)\tau^6, \quad \mu = 0, 1. \quad (3.7)$$

3.2. The cubic MARS algorithm. We adopt the cubic MARS algorithm in [26] which constructs a C^2 -smooth boundary with cubic spline interpolation. The purpose here is to estimate the error between the exact boundary and the approximate boundary.

Let L_0 be the curve length of Γ_0 . Suppose Γ_0 has a parametrization

$$\Gamma_0 = \{\boldsymbol{\chi}_0(l) : l \in [0, L_0]\}, \quad \boldsymbol{\chi}_0 \in \mathbf{C}^4([0, L_0]). \quad (3.8)$$

The interface tracking algorithm starts with a uniform partition, $\mathcal{L}^0 = \{l_j = j\eta : j = 0, 1, \dots, J_0\}$, $\eta = L_0/J_0$, of the interval $[0, L_0]$ and a set of markers $\mathcal{P}^0 = \{\mathbf{p}_j^0 := \boldsymbol{\chi}_0(l_j) : 0 \leq j \leq J_0\}$.

ALGORITHM 3.1. *Given $\Gamma_\eta^0 := \Gamma_0$ and its nodal set $\mathcal{L}^0 = \{l_j^0 := l_j : 0 \leq j \leq J_0\}$ and marker set \mathcal{P}^0 , the cubic MARS algorithm for constructing Γ_η^n , $n \geq 1$, consists of four steps.*

1. Trace forward each marker in \mathcal{P}^{n-1} to obtain the set of markers at $t = t_n$,

$$\mathcal{P}^n = \{\mathbf{p}_j^n = \mathbf{X}_\tau^{n-1,n}(\mathbf{p}_j^{n-1}) : j = 1, \dots, J_{n-1}\}, \quad J_n = J_{n-1}.$$

2. Adjust the set of markers \mathcal{P}^n .

- If $M_j := \lceil |\mathbf{p}_j^n - \mathbf{p}_{j-1}^n| / \eta \rceil > 1$, create new markers on Γ_η^{n-1}

$$\mathbf{p}_{j,m}^{n-1} = \boldsymbol{\chi}_{n-1}(l_{j-1}^{n-1} + m(l_j^{n-1} - l_{j-1}^{n-1})/M_j), \quad 1 \leq m < M_j,$$

and update \mathcal{P}^n as follows

$$\mathcal{P}^n \leftarrow \mathcal{P}^n \cup \{\mathbf{X}_\tau^{n-1,n}(\mathbf{p}_{j,m}^{n-1}) : 1 \leq m < M_j\}, \quad J_n \leftarrow J_n + M_j - 1. \quad (3.9)$$

- Remove markers from $\mathcal{P}^n \setminus \mathbf{X}_\tau^{0,n}(\mathcal{P}^0)$ such that

$$0.1\eta < |\mathbf{p}_{j+1}^n - \mathbf{p}_j^n| \leq \eta, \quad j = 0, \dots, J_n.$$

3. Construct $\mathcal{L}^n = \{l_j^n : 0 \leq j \leq J_n\}$ where $l_0^n = 0$ and $l_j^n = l_{j-1}^n + |\mathbf{p}_j^n - \mathbf{p}_{j-1}^n|$.
4. Compute the cubic spline function $\boldsymbol{\chi}_n \in \mathbf{C}^2([0, L_n])$, where $L_n := l_{J_n}^n$, based on the nodal set \mathcal{L}^n and the marker set \mathcal{P}^n (see Fig. 3.1). Construct the approximate boundary by

$$\Gamma_\eta^n := \{\boldsymbol{\chi}_n(l) : l \in [0, L_n]\}. \quad (3.10)$$

REMARK 3.2. *The use of cubic spline function in constructing Γ_η^n has two benefits. 1) The explicit expression of $\boldsymbol{\chi}_n$ makes the computation of integrals on cut elements very efficient. 2) The C^2 -smoothness of Γ_η^n admits a duality argument in L^2 -finite element error estimates.*

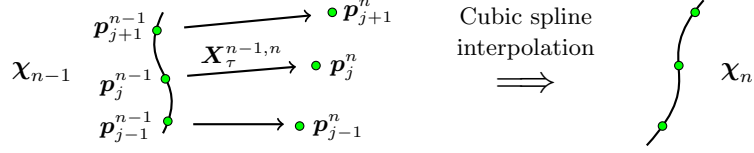


Fig. 3.1: An illustration of the interface tracking.

3.3. Error estimate for the approximate boundary. Now we estimate the difference between the approximate boundary Γ_η^n and the exact boundary Γ_{t_n} . *The theories of this subsection are restricted to the case without Step 2 in Algorithm 3.1.* Here we emphasize that this restriction on Algorithm 3.1 is only required for theoretical analyses, not for numerical computations.

ASSUMPTION 3.3. *In theoretical analyses of this paper, we let $\chi_n \in C^2([0, L_0])$ be the cubic spline function computed with the marker set $\mathcal{P}^n = \{\mathbf{p}_j^n = \mathbf{X}_\tau^{0,n}(\mathbf{p}_j^0) : 0 \leq j \leq J_0\}$ and the initial nodal set \mathcal{L}^0 . Moreover, the segment size for interface tracking satisfies $\eta = O(\tau^{5/4})$.*

Assumption 3.3 indicates that our theories only apply to the case that Γ_t has mild deformations. Remember that the exact boundary is given by

$$\Gamma_{t_n} = \{\hat{\chi}_n(l) : 0 \leq l \leq L_0\}, \quad \hat{\chi}_n := \mathbf{X}^{0,n} \circ \chi_0. \quad (3.11)$$

Assumption 2.1 implies $\|\hat{\chi}_n\|_{C^4([0, L_0])} \lesssim 1$ for all $0 \leq n \leq N$. By (3.2) and (3.6), the arc length of Γ_{t_n} between $\mathbf{X}^{0,n}(\mathbf{p}_{j-1}^0)$ and $\mathbf{X}^{0,n}(\mathbf{p}_j^0)$ satisfies

$$\int_{l_{j-1}}^{l_j} |\hat{\chi}'_n| = \int_{l_{j-1}}^{l_j} |\mathbb{J}^{0,n} \chi'_0| \lesssim \eta, \quad \eta = \int_{l_{j-1}}^{l_j} |\chi'_0| \lesssim \int_{l_{j-1}}^{l_j} |\mathbb{J}^{n,0} \hat{\chi}'_n| \lesssim \int_{l_{j-1}}^{l_j} |\hat{\chi}'_n|.$$

This means that $\mathbf{X}^{0,n}(\mathcal{P}_0)$ provides a quasi-uniform partition of Γ_{t_n} . Intuitively, the approximation of Γ_{t_n} with Γ_η^n does not deteriorate if we use $\mathcal{P}^n = \mathbf{X}^{0,n}(\mathcal{P}_0)$.

Based on the uniform partition \mathcal{L}^0 of $[0, L_0]$, χ_n can be written explicitly as follows

$$\chi_n(l) = \sum_{j=1}^{J_0} [\mathbf{p}_j^n b_j + \boldsymbol{\alpha}_j^n b_j (b_j^2 - 1)], \quad \boldsymbol{\alpha}_0 = \boldsymbol{\alpha}_{J_0}, \quad (3.12)$$

where $b_j \in C([0, L_0])$ is linear on each sub-interval $[l_{i-1}, l_i]$ and satisfies $b_j(l_i) = \delta_{i,j}$. Define $\underline{\mathbf{d}}^n = [\mathbf{d}_1^n, \dots, \mathbf{d}_{J_0}^n]^\top$ with $\mathbf{d}_j^n = \mathbf{p}_{j+1}^n + \mathbf{p}_{j-1}^n - 2\mathbf{p}_j^n$ and $\mathbf{p}_{J_0+1}^n = \mathbf{p}_1^n$. The coefficient tensor $\underline{\boldsymbol{\alpha}}^n = [\boldsymbol{\alpha}_1^n, \dots, \boldsymbol{\alpha}_{J_0}^n]^\top$ solves the system of algebraic equations

$$\mathbb{G} \underline{\boldsymbol{\alpha}}^n = \underline{\mathbf{d}}^n, \quad (3.13)$$

where \mathbb{G} is the $(2J_0) \times (2J_0)$ matrix

$$\mathbb{G} = \begin{bmatrix} 4 & 0 & 1 & & & 1 & 0 \\ 0 & 4 & 0 & 1 & & & 1 \\ 1 & 0 & 4 & 0 & 1 & & \\ & \ddots & \ddots & \ddots & \ddots & \ddots & \\ & & 1 & 0 & 4 & 0 & 1 \\ 1 & & & 1 & 0 & 4 & 0 \\ 0 & 1 & & & 1 & 0 & 4 \end{bmatrix}. \quad (3.14)$$

To measure the difference between Γ_η^n and Γ_{t_n} , it suffices to estimate the error $\boldsymbol{\chi}_n - \hat{\boldsymbol{\chi}}_n$.

LEMMA 3.4. *Let Assumptions 2.1 and 3.3 be satisfied. Then*

$$\|\boldsymbol{\chi}_n - \hat{\boldsymbol{\chi}}_n\|_{\mathcal{C}^\mu([0, L_0])} \lesssim \eta^{4-\mu} + \tau^5, \quad 0 \leq n \leq N, \quad \mu = 0, 1, 2. \quad (3.15)$$

Proof. Define $\tilde{\boldsymbol{\chi}}_n(l) := \mathbf{X}_\tau^{0,n}(\boldsymbol{\chi}_0(l))$. Clearly $\boldsymbol{\chi}_n$ is the cubic spline interpolation of $\tilde{\boldsymbol{\chi}}_n$. By the chain rule, (3.5), and standard error estimates for cubic spline interpolations, we have

$$\|\tilde{\boldsymbol{\chi}}_n\|_{\mathcal{C}^4([0, L_0])} \lesssim 1, \quad \|\boldsymbol{\chi}_n - \tilde{\boldsymbol{\chi}}_n\|_{\mathcal{C}^\mu([0, L_0])} \lesssim \eta^{4-\mu}. \quad (3.16)$$

The proof is finished by using the triangular inequality and (3.7). \square

THEOREM 3.5. *Let $\eta = O(\tau^{5/4})$. The composite function $\mathbf{X}_\tau^{m,n} \circ \boldsymbol{\chi}_m(l) = \mathbf{X}_\tau^{m,n}(\boldsymbol{\chi}_m(l))$ satisfies*

$$\|\boldsymbol{\chi}_n - \mathbf{X}_\tau^{m,n} \circ \boldsymbol{\chi}_m\|_{\mathcal{C}^\mu([0, L_0])} \lesssim \tau^{6-5\mu/4}, \quad 0 \leq n - m \leq 4, \quad \mu = 0, 1. \quad (3.17)$$

Proof. First we estimate $\boldsymbol{\chi}_n - \boldsymbol{\chi}_m$. For fixed $s \geq 0$ and \mathbf{p} , we define a univariate function of t by $\mathbf{W}(t; s, \mathbf{p}) := \mathbf{w}(\mathbf{X}(t; s, \mathbf{p}), t)$. Let $\mathbf{W}^{(i)}(t; s, \mathbf{p})$ denote the i^{th} -order derivative of $\mathbf{W}(t; s, \mathbf{p})$ with respect to t . Assumption 2.1 and the chain rule show that

$$|\mathbf{W}^{(1)}(t; s, \mathbf{p})| = \left| (\mathbf{w} \cdot \nabla \mathbf{w})(\mathbf{X}(t; s, \mathbf{p}), t) + \frac{\partial \mathbf{w}}{\partial t}(\mathbf{X}(t; s, \mathbf{p}), t) \right| \lesssim 1.$$

High-order derivatives of $\mathbf{W}(\cdot; s, \mathbf{p})$ can be estimated similarly. Using (2.3), we have

$$\|\mathbf{X}(\cdot; s, \mathbf{p})\|_{\mathcal{C}^7([s, T])} + \|\mathbf{W}(\cdot; s, \mathbf{p})\|_{\mathcal{C}^6([s, T])} \lesssim 1.$$

By (3.7) and Taylor's expansion of $\mathbf{X}(t_n; t_m, \mathbf{p})$ at t_m , we have

$$\mathbf{X}_\tau^{m,n}(\mathbf{p}) = \mathbf{X}(t_n; t_m, \mathbf{p}) + O(\tau^6) = \mathbf{p} + \sum_{i=0}^4 \frac{\mathbf{W}^{(i)}(t_m; t_m, \mathbf{p})}{(i+1)!} (t_n - t_m)^{i+1} + O(\tau^6). \quad (3.18)$$

Since $\|\mathbb{G}^{-1}\|_\infty \lesssim 1$, taking $\mathbf{p} = \mathbf{p}_j^n \equiv \mathbf{X}_\tau^{m,n}(\mathbf{p}_j^m)$ in (3.18) and using the definitions of \mathbf{d}_j^n and \mathbf{d}_j^m , we find that

$$\underline{\boldsymbol{\alpha}}^n - \underline{\boldsymbol{\alpha}}^m = \mathbb{G}^{-1}(\underline{\mathbf{d}}^n - \underline{\mathbf{d}}^m) = \sum_{i=0}^4 \frac{(t_n - t_m)^{i+1}}{(i+1)!} \underline{\gamma}_i + O(\tau^6), \quad (3.19)$$

where $\underline{\gamma}_i = \mathbb{G}^{-1}\underline{\beta}_i$ and $\underline{\beta}_i = [\beta_{i,1}, \dots, \beta_{i,J_0}]^\top$. Each component of $\underline{\beta}_i$ is defined as

$$\beta_{i,j} = \mathbf{W}^{(i)}(t_m; t_m, \mathbf{p}_{j+1}^m) + \mathbf{W}^{(i)}(t_m; t_m, \mathbf{p}_{j-1}^m) - 2\mathbf{W}^{(i)}(t_m; t_m, \mathbf{p}_j^m),$$

where $\mathbf{p}_{J_0+1}^m := \mathbf{p}_1^m$. Using the equality $|b'_j| = \eta^{-1}$ and (3.12), we immediately get

$$\chi_n^{(\mu)} - \chi_m^{(\mu)} = \sum_{i=0}^4 \frac{(t_n - t_m)^{i+1}}{(i+1)!} \zeta_i^{(\mu)} + O(\eta^{-\mu}\tau^6), \quad \mu = 0, 1, \quad (3.20)$$

where $\zeta_i = \sum_{j=1}^{J_0} [\mathbf{W}^{(i)}(t_m; t_m, \mathbf{p}_j^m)b_j + \gamma_{i,j}b_j(b_j^2 - 1)]$ is a cubic spline function on $[0, L_0]$.

Note from (3.16) that $\tilde{\chi}_m = \mathbf{X}_\tau^{0,m} \circ \chi_0 \in \mathbf{C}^4([0, L_0])$ and $\mathbf{w} \in \mathbf{C}^6(\mathbb{R}^2 \times [0, T])$. For $0 \leq i \leq 4$, $\mathbf{W}^{(i)}(t_m; t_m, \tilde{\chi}_m)$ defines a function in $\mathbf{C}^{\min(4, 6-i)}([0, L_0])$. Moreover, since

$$\tilde{\chi}_m(l_j) = \mathbf{X}_\tau^{0,m}(\chi_0(l_j)) = \mathbf{X}_\tau^{0,m}(\mathbf{p}_j^0) = \mathbf{p}_j^m, \quad 0 \leq j \leq J_0,$$

ζ_i is actually the cubic spline interpolation of $\mathbf{W}^{(i)}(t_m; t_m, \tilde{\chi}_m)$. Standard error estimates yield

$$\|\zeta_i - \mathbf{W}^{(i)}(t_m; t_m, \tilde{\chi}_m)\|_{\mathbf{C}^\mu([0, L_0])} \lesssim \eta^{-\mu} \eta^{\min(4, 6-i)} \lesssim \eta^{-\mu} (\tau^5 + \tau^{7.5-1.25i}), \quad (3.21)$$

where we have used the relation $\eta = O(\tau^{5/4})$. Combining (3.20) and (3.21) yields

$$\chi_n^{(\mu)} - \chi_m^{(\mu)} = \sum_{i=0}^4 \frac{(t_n - t_m)^{i+1}}{(i+1)!} \frac{d^\mu}{dl^\mu} \mathbf{W}^{(i)}(t_m; t_m, \tilde{\chi}_m) + O(\eta^{-\mu}\tau^6), \quad \mu = 0, 1. \quad (3.22)$$

Applying (3.18) to $\mathbf{X}_\tau^{m,n}(\chi_m)$ and using (3.22) and (3.16), we find that

$$|\chi_n - \mathbf{X}_\tau^{m,n} \circ \chi_m| \lesssim \sum_{i=0}^4 \tau^{i+1} |\mathbf{W}^{(i)}(t_m; t_m, \tilde{\chi}_m) - \mathbf{W}^{(i)}(t_m; t_m, \chi_m)| + \tau^6 \lesssim \tau^6.$$

Since $\mathbf{w} \in \mathbf{C}^6(\mathbb{R}^2 \times [0, T])$, similar to (3.18), we also have

$$\nabla_{\mathbf{p}} \mathbf{X}_\tau^{m,n}(\mathbf{p}) = \mathbb{I} + \sum_{i=0}^4 \frac{(t_n - t_m)^{i+1}}{(i+1)!} \nabla_{\mathbf{p}} \mathbf{W}^{(i)}(t_m; t_m, \mathbf{p}) + O(\tau^6).$$

Using (3.22) and (3.16), the derivative of $\chi_n - \mathbf{X}_\tau^{m,n} \circ \chi_m$ can be estimated similarly

$$\begin{aligned} |\chi'_n - (\mathbf{X}_\tau^{m,n} \circ \chi_m)'| &\lesssim \sum_{i=0}^4 \tau^{i+1} \left| \frac{d}{dl} \mathbf{W}^{(i)}(t_m; t_m, \tilde{\chi}_m) - \frac{d}{dl} \mathbf{W}^{(i)}(t_m; t_m, \chi_m) \right| + \eta^{-1}\tau^6 \\ &\lesssim \sum_{i=0}^4 \tau^{i+1} |\tilde{\chi}'_m - \chi'_m| + \eta^{-1}\tau^6 \lesssim \eta^{-1}\tau^6. \end{aligned}$$

The proof is finished by using $\eta = O(\tau^{5/4})$. \square

4. The unfitted characteristic finite element method. The purpose of this section is to propose the UCFEM for solving (2.1) on a fixed mesh. First we take an open square $D \subset \mathbb{R}^2$ which is large enough such that $\Omega_t \cup \Omega_\eta^n \subset D$ for all $0 \leq t \leq T$ and $0 \leq n \leq N$.

4.1. Finite element spaces. Let \mathcal{T}_h be the uniform partition of \bar{D} into *closed* squares of side-length h . Let $\Omega_\eta^n \subset D$ be a domain slightly larger than Ω_η^n :

$$\tilde{\Omega}_\eta^n := \{\mathbf{x} \in \mathbb{R}^2 : \text{dist}(\mathbf{x}, \overline{\Omega_\eta^n}) < h/2\}, \quad \tilde{\Gamma}_\eta^n := \partial\tilde{\Omega}_\eta^n \quad (4.1)$$

Clearly \mathcal{T}_h generates a cover of $\tilde{\Omega}_\eta^n$ and a cover of $\Gamma_\eta^n \cup \tilde{\Gamma}_\eta^n$, respectively, (see Fig. 4.1)

$$\begin{aligned} \mathcal{T}_h^n &:= \left\{ K \in \mathcal{T}_h : \text{area}(K \cap \tilde{\Omega}_\eta^n) > 0 \right\}, \\ \mathcal{T}_{h,B}^n &:= \left\{ K \in \mathcal{T}_h^n : \text{length}(K \cap \Gamma_\eta^n) > 0 \text{ or } \text{length}(K \cap \tilde{\Gamma}_\eta^n) > 0 \right\}. \end{aligned}$$

Then \mathcal{T}_h^n generates a polygonal domain Ω_h^n which contains $\tilde{\Omega}_\eta^n$:

$$\Omega_h^n := \text{interior}\left(\cup_{K \in \mathcal{T}_h^n} K\right), \quad \Gamma_h^n := \partial\Omega_h^n.$$

Let \mathcal{E}_h be the set of all edges in \mathcal{T}_h and define

$$\mathcal{E}_{h,B}^n = \left\{ E \in \mathcal{E}_h : E \not\subset \Gamma_h^n \text{ and } \exists K \in \mathcal{T}_{h,B}^n \text{ s.t. } E \subset \partial K \right\}.$$

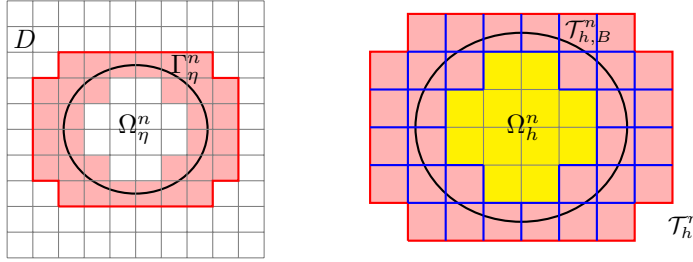


Fig. 4.1: Left: the square domain D and its partition \mathcal{T}_h , the approximate boundary Γ_η^n , and the approximate domain Ω_η^n surrounded by Γ_η^n . Right: the set of red and yellow squares \mathcal{T}_h^n , the set of red squares $\mathcal{T}_{h,B}^n$, the set of blue edges $\mathcal{E}_{h,B}^n$, and $\tilde{\Omega}_\eta^n =$ the union of red and yellow squares.

The finite element spaces on D and on Ω_h^n are, respectively, defined as

$$V_h := \{v \in H^1(D) : v|_K \in Q_4(K), \forall K \in \mathcal{T}_h\}, \quad V_h^n := \{v|_{\Omega_h^n} : v \in V_h\},$$

where Q_4 is the space of polynomials whose degrees are no more than 4 for each variable. The space of piecewise regular functions over \mathcal{T}_h^n is defined as

$$H^m(\mathcal{T}_h^n) := \{v \in L^2(\Omega_h^n) : v|_K \in H^m(K), \forall K \in \mathcal{T}_h^n\}, \quad m \geq 1.$$

Throughout the paper, we extend $v_h \in V_h^n$ to the exterior of Ω_h^n such that the extension, denoted still by v_h , belongs to V_h and vanishes at degrees of freedom outside of $\tilde{\Omega}_\eta^n$. It is easy to see that

$$\|v_h\|_{L^2(D)} \lesssim \|v_h\|_{L^2(\Omega_h^n)}, \quad \|v_h\|_{H^1(D)} \lesssim \|v_h\|_{H^1(\Omega_h^n)}. \quad (4.2)$$

4.2. The discrete problem. We define four bilinear forms on $H^5(\mathcal{T}_h^n) \cap H^1(\Omega_h^n)$ as follows

$$\mathcal{A}_h^n(w, v) := (\nabla w, \nabla v)_{\Omega_\eta^n} + \mathcal{S}_h^n(w, v) + \mathcal{J}_0^n(w, v) + \mathcal{J}_1^n(w, v), \quad (4.3)$$

$$\mathcal{S}_h^n(w, v) := - \int_{\Gamma_\eta^n} (v \partial_{\mathbf{n}} w + w \partial_{\mathbf{n}} v), \quad (4.4)$$

$$\mathcal{J}_0^n(w, v) := \frac{\gamma_0}{h} \int_{\Gamma_\eta^n} wv, \quad (4.5)$$

$$\mathcal{J}_1^n(w, v) := \gamma_1 \sum_{E \in \mathcal{E}_{h,E}^n} \sum_{l=1}^4 h^{2l-1} \int_E \llbracket \partial_{\mathbf{n}}^l w \rrbracket \llbracket \partial_{\mathbf{n}}^l v \rrbracket, \quad (4.6)$$

where γ_0, γ_1 are positive constants and $\partial_{\mathbf{n}} v$ denotes the normal derivative of v on Γ_η^n . In (4.6), $\partial_{\mathbf{n}}^l v$ denotes the l -th order normal derivative of v on E and $\llbracket \partial_{\mathbf{n}}^l v \rrbracket$ denotes the jump of $\partial_{\mathbf{n}}^l v$ across E . Here \mathcal{J}_0^n is used to impose the Dirichlet boundary condition of u_h^n weakly, \mathcal{J}_1^n is used to enhance the stability of u_h^n (see section 5). Moreover, $(\cdot, \cdot)_{\Omega_\eta^n}$ stands for the inner product on $L^2(\Omega_\eta^n)$.

The UCFEM for (2.1) is to seek $u_h^n \in V_h^n$ such that

$$\frac{1}{\tau} \sum_{i=0}^4 \lambda_i (U_h^{n-i,n}, v_h)_{\Omega_\eta^n} + \mathcal{A}_h^n(u_h^n, v_h) = (f^n, v_h)_{\Omega_\eta^n} \quad \forall v_h \in V_h^n, \quad (4.7)$$

where $(\lambda_0, \lambda_1, \lambda_2, \lambda_3, \lambda_4) = (25/12, -4, 3, -4/3, 1/4)$, $f^n = f(t_n)$, and

$$U_h^{n-i,n}(\mathbf{x}) := (u_h^{n-i} \circ \mathbf{X}_\tau^{n,n-i})(\mathbf{x}) = u_h^{n-i}(\mathbf{X}_\tau^{n,n-i}(\mathbf{x})). \quad (\text{see Fig. 4.2})$$

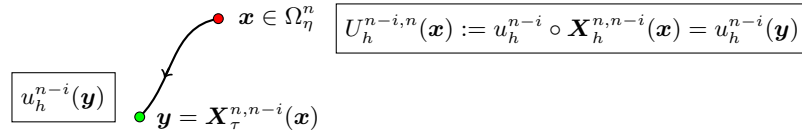


Fig. 4.2: An illustration of $U_h^{n-i,n}(\mathbf{x})$: calculate $\mathbf{y} = \mathbf{X}_\tau^{n,n-i}(\mathbf{x})$ and evaluate $u_h^{n-i}(\mathbf{y})$.

4.3. Some discussions of quadratures. Numerical solutions of PDEs on moving domains are usually time-consuming due to quadratures on “irregular domains” or “cut elements”. The issue becomes even more extrusive for high-order methods than low-order methods. Now we explain that the quadratures in our method can be done efficiently.

The most time-consuming computations involve the first term on the left-hand side of (4.7):

$$\int_{\Omega_\eta^n} U_h^{n-i,n} v_h = \sum_{K \in \mathcal{T}_h^n} \int_{K \cap \Omega_\eta^n} U_h^{n-i,n} v_h, \quad 0 \leq i \leq 4, \quad v_h \in V_h^n.$$

We consider the quadratures on interior elements and boundary elements, respectively.

1. *Quadratures on interior elements* The integrand $U_h^{n-i,n} v_h$ is continuous and piecewise smooth on any interior element $K \subset \Omega_\eta^n$. We compute $\int_K U_h^{n-i,n} v_h$ directly with the $(2k+3)$ th-order Gauss-Legendre quadrature on K .

2. *Quadratures on cut elements.* Suppose $K \in \mathcal{T}_{h,B}^n$. Since Γ_η^n is constructed with Algorithm 3.1, the curved edges $K \cap \Gamma_\eta^n$ are represented explicitly by the piecewise cubic function χ_n . Therefore, $K \cap \Omega_\eta^n$ can be easily subdivided into the union of several X-type and Y-type sub-regions (see Fig. 4.3). We compute the integral on each sub-region with the $(2k+3)$ th-order Gauss-Legendre quadrature.

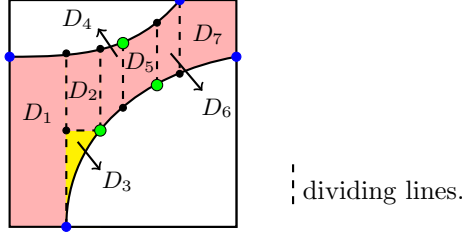


Fig. 4.3: The partition of a cut element: $K \cap \Omega_\eta^n = \bigcup_{i=1}^7 D_i$. Each sub-region D_i is of either X-type or Y-type (D_3 is of Y-type and the others are of X-type). Each dividing line has at least one endpoint being a marker (green point) or an intersection point of $\Gamma_\eta^n \cap \partial K$ (blue point).

4.4. The well-posedness of (4.7). Now we prove that the discrete problem (4.7) has a unique solution in each time step. First we make a mild assumption on the finite element mesh. It can be satisfied if \mathcal{T}_h is fine and the deformation of the domain is moderate.

ASSUMPTION 4.1. *There exist an integer $I > 0$ and a $\gamma > 0$ which are independent of h and τ , such that, for any $K \in \mathcal{T}_{h,B}^n$, one can find at most I elements $\{K_j\}_{j=1}^I \subset \mathcal{T}_h^n$ satisfying $K_1 = K$, $K_{j-1} \cap K_j \in \mathcal{E}_{h,B}^n$ for $1 < j \leq I$, and that $K_I \cap \Omega_\eta^n$ contains a disk of radius γh (see Fig. 4.4).*

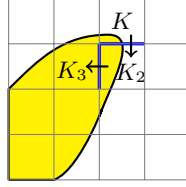


Fig. 4.4: An illustration of Assumption 4.1 for $I = 3$: K_3 contains a disk of radius γh .

To prove the well-posedness of (4.7), we define the mesh-dependent norms

$$\|v\|_{\Omega_\eta^n} = (|v|_{H^1(\Omega_\eta^n)}^2 + h^{-1} \|v\|_{L^2(\Gamma_\eta^n)}^2 + h \|\partial_n v\|_{L^2(\Gamma_\eta^n)}^2)^{1/2},$$

$$\|v\|_{\mathcal{T}_h^n} = (|v|_{H^1(\Omega_\eta^n)}^2 + \mathcal{J}_0^n(v, v) + \mathcal{J}_1^n(v, v))^{1/2},$$

$$\|v\|_{*, \Omega_\eta^n} = (|v|_{H^1(\Omega_\eta^n)}^2 + h^{-1} \|v\|_{L^2(\Gamma_\eta^n)}^2)^{1/2}.$$

LEMMA 4.2. *Let Assumption 4.1 be satisfied. Then for any $v_h \in V_h^n$,*

$$\|v_h\|_{L^2(\Omega_\eta^n)}^2 \lesssim \|v_h\|_{L^2(\Omega_\eta^n)}^2 + h^2 \mathcal{J}_1^n(v_h, v_h), \quad (4.8)$$

$$\|v_h\|_{\Omega_\eta^n} \lesssim \|v_h\|_{\mathcal{T}_h^n} \approx \|v_h\|_{*, \Omega_\eta^n}. \quad (4.9)$$

Proof. For each $K \in \mathcal{T}_{h,B}^n$, by Assumption 4.1, there exist (at most) I elements $K_1 = K, K_2, \dots, K_I$ such that $E_j = K_{j-1} \cap K_j \in \mathcal{E}_{h,B}^n$, $1 < j \leq I$, and that $K_I \cap \Omega_\eta^n$ contains a disk of radius γh . By [20, Lemma 5.1], we have

$$\|\nabla^\mu v_h\|_{\mathbf{L}^2(K_{j-1})}^2 \lesssim \|\nabla^\mu v_h\|_{\mathbf{L}^2(K_j)}^2 + \sum_{l=1}^4 h^{2(l-\mu)+1} \int_{E_j} \llbracket \partial_{\mathbf{n}}^l v_h \rrbracket^2, \quad \mu = 0, 1.$$

Since $K_I \cap \Omega_\eta^n$ contains a disk of radius γh , the norm equivalence shows

$$\|\nabla^\mu v_h\|_{\mathbf{L}^2(K)}^2 \lesssim \|\nabla^\mu v_h\|_{\mathbf{L}^2(K_I \cap \Omega_\eta^n)}^2 + \sum_{j=2}^I \sum_{l=1}^4 h^{2(l-\mu)+1} \int_{E_j} \llbracket \partial_{\mathbf{n}}^l v_h \rrbracket^2, \quad \mu = 0, 1. \quad (4.10)$$

Take the sum of (4.10) over all $K \in \mathcal{T}_{h,B}^n$. Letting $\mu = 0$ shows (4.8) and letting $\mu = 1$ shows

$$|v_h|_{H^1(\Omega_\eta^n)}^2 \lesssim |v_h|_{H^1(\Omega_\eta^n)}^2 + \mathcal{J}_1^n(v_h, v_h). \quad (4.11)$$

Then we have $\|v_h\|_{*,\Omega_\eta^n} \lesssim \|v_h\|_{\mathcal{T}_h^n}$. Inverse estimates also yield $\mathcal{J}_1^n(v_h, v_h) \lesssim |v_h|_{H^1(\Omega_\eta^n)}^2$. This shows $\|v_h\|_{\mathcal{T}_h^n} \approx \|v_h\|_{*,\Omega_\eta^n}$. The proof of $\|v_h\|_{\Omega_\eta^n} \lesssim \|v_h\|_{*,\Omega_\eta^n}$ is similar. \square

THEOREM 4.3. *Let Assumption 4.1 be satisfied and suppose γ_0 is large enough. Problem (4.7) has a unique solution $u_h^n \in V_h^n$ in each time step.*

Proof. From [9, Lemma 1 and Appendix A], we have the trace inequality, for any $K \in \mathcal{T}_h^n$,

$$\|v\|_{L^2(\partial K)} + \|v\|_{L^2(K \cap \Gamma_\eta^n)} \lesssim h^{-1/2} \|v\|_{L^2(K)} + h^{1/2} |v|_{H^1(K)}, \quad \forall v \in H^1(K). \quad (4.12)$$

Using the Cauchy-Schwarz inequality, it is standard to show the coercivity and continuity of \mathcal{A}_h^n :

$$\mathcal{A}_h^n(v_h, v_h) \gtrsim \|v_h\|_{\mathcal{T}_h^n}^2, \quad |\mathcal{A}_h^n(u_h, v_h)| \lesssim \|u_h\|_{\mathcal{T}_h^n} \|v_h\|_{\mathcal{T}_h^n}, \quad \forall u_h, v_h \in V_h^n. \quad (4.13)$$

The details are omitted here. The Lax-Milgram lemma shows that (4.7) has a unique solution. \square

5. The stability of numerical solutions. The core difficulty in proving stability and convergence is the fact that $U_h^{n-i,n} = u_h^{n-i} \circ \mathbf{X}_\tau^{n,n-i} \notin V_h^n$; we overcome this difficulty by introducing a modified Ritz projection operator that projects $U_h^{n-i,n}$ into V_h^n .

5.1. The modified Ritz projection. It is easy to see that

$$U_h^{n-i,n} \in Y(\Omega_\eta^n) := \{v \in H^1(\Omega_\eta^n) : \|v\|_{\Omega_\eta^n} < \infty\}, \quad 0 \leq i \leq 4. \quad (5.1)$$

The modified Ritz projection operator $\mathcal{P}_h^n : Y(\Omega_\eta^n) \rightarrow V_h^n$ is defined as

$$\mathcal{A}_h^n(\mathcal{P}_h^n w, v_h) = a_h^n(w, v_h), \quad \forall v_h \in V_h^n, \quad (5.2)$$

where $a_h^n(w, v) := \mathcal{A}_h^n(w, v) - \mathcal{J}_1^n(w, v)$. By (4.13), Lemma 4.2, and standard techniques for finite element error estimates, it is easy to prove the results

$$\|\mathcal{P}_h^n v\|_{\Omega_\eta^n} + \|\mathcal{P}_h^n v\|_{\mathcal{T}_h^n} \lesssim \|v\|_{\Omega_\eta^n}, \quad \forall v \in Y(\Omega_\eta^n), \quad (5.3)$$

$$\|w - \mathcal{P}_h^n w\|_{\Omega_\eta^n} + \|w - \mathcal{P}_h^n w\|_{\mathcal{T}_h^n} + \|w - \mathcal{P}_h^n w\|_{*,\Omega_\eta^n} \lesssim h^4 |w|_{H^5(D)}, \quad \forall w \in H^5(D). \quad (5.4)$$

Below we only prove the L^2 -error estimates by duality argument.

LEMMA 5.1. *Suppose Assumption 4.1 holds. Then*

$$\|v - \mathcal{P}_h^n v\|_{L^2(\Omega_\eta^n)} \lesssim h \|v\|_{\Omega_\eta^n}, \quad \forall v \in Y(\Omega_\eta^n), \quad (5.5)$$

$$\|v - \mathcal{P}_h^n v\|_{L^2(\Omega_\eta^n)} \lesssim h^5 |v|_{H^5(\Omega_\eta^n)}, \quad \forall v \in H^5(\Omega_\eta^n). \quad (5.6)$$

Proof. Consider the auxiliary problem

$$-\Delta z = v - \mathcal{P}_h^n v \quad \text{in } \Omega_\eta^n, \quad z = 0 \quad \text{on } \Gamma_\eta^n. \quad (5.7)$$

By Theorem 3.4, Γ_η^n is C^2 -smooth and its parametrization satisfies $\|\chi_n\|_{C^2([0,L])} \lesssim 1$. The regularity result for elliptic equations yields $\|z\|_{H^2(\Omega_\eta^n)} \leq C \|v - \mathcal{P}_h^n v\|_{L^2(\Omega_\eta^n)}$.

Multiplying both sides of the equation with $v - \mathcal{P}_h^n v$ and integrating by parts, we have

$$\|v - \mathcal{P}_h^n v\|_{L^2(\Omega_\eta^n)}^2 = \int_{\Omega_\eta^n} \nabla z \cdot \nabla (v - \mathcal{P}_h^n v) - \int_{\Gamma_\eta^n} \frac{\partial z}{\partial \mathbf{n}} (v - \mathcal{P}_h^n v) = a_h(v - \mathcal{P}_h^n v, z). \quad (5.8)$$

Let $\tilde{z} \in H^2(D)$ be the Sobolev extension of z to the exterior of Ω_η^n [23]. There is a constant C depending only on Ω_η^n such that $\|\tilde{z}\|_{H^2(D)} \leq C \|z\|_{H^2(\Omega_\eta^n)} \leq C \|v - \mathcal{P}_h^n v\|_{L^2(\Omega_\eta^n)}$. Let \tilde{z}_h be the linear Scott-Zhang interpolation of \tilde{z} on the mesh \mathcal{T}_h . From [22] and using (4.12), we have

$$\|\tilde{z} - \tilde{z}_h\|_{\Omega_\eta^n}^2 + \sum_{E \in \mathcal{E}_{h,B}^n} h \int_E \llbracket \partial_{\mathbf{n}}(\tilde{z} - \tilde{z}_h) \rrbracket^2 \lesssim h^2 \|\tilde{z}\|_{H^2(D)}^2 \lesssim h^2 \|v - \mathcal{P}_h^n v\|_{L^2(\Omega_\eta^n)}^2. \quad (5.9)$$

Inserting the equality $a_h(v - \mathcal{P}_h^n v, \tilde{z}_h) = \mathcal{J}_1^n(\mathcal{P}_h^n v, \tilde{z}_h)$ into (5.8) shows

$$\|v - \mathcal{P}_h^n v\|_{L^2(\Omega_\eta^n)}^2 = a_h(v - \mathcal{P}_h^n v, \tilde{z} - \tilde{z}_h) + \mathcal{J}_1^n(\mathcal{P}_h^n v, \tilde{z}_h). \quad (5.10)$$

Applying (5.3) and (5.9) shows that

$$a_h(v - \mathcal{P}_h^n v, \tilde{z} - \tilde{z}_h) \lesssim \|v - \mathcal{P}_h^n v\|_{\Omega_\eta^n} \|\tilde{z} - \tilde{z}_h\|_{\Omega_\eta^n} \lesssim h \|v\|_{\Omega_\eta^n} \|v - \mathcal{P}_h^n v\|_{L^2(\Omega_\eta^n)}. \quad (5.11)$$

For each $E \in \mathcal{E}_{h,B}^n$, $\tilde{z}_h|_E$ is a linear function of either x or y . By (5.9) and (5.3), we have

$$|\mathcal{J}_1^n(\mathcal{P}_h^n v, \tilde{z}_h)| = \left| \sum_{E \in \mathcal{E}_{h,B}^n} h \int_E \llbracket \partial_{\mathbf{n}}(\mathcal{P}_h^n v) \rrbracket \llbracket \partial_{\mathbf{n}}(\tilde{z}_h - \tilde{z}) \rrbracket \right| \lesssim h \|v\|_{\Omega_\eta^n} \|v - \mathcal{P}_h^n v\|_{L^2(\Omega_\eta^n)}. \quad (5.12)$$

We get (5.5) by inserting (5.11) and (5.12) into (5.10).

Next let $\tilde{v} \in H^5(D)$ be the Sobolev extension of $v \in H^5(\Omega_\eta^n)$. Then $\llbracket \partial_{\mathbf{n}} \tilde{v} \rrbracket = 0$ on each $E \in \mathcal{E}_{h,B}^n$. Applying (5.10), (5.9), and (5.4) sequentially, we find that

$$\begin{aligned} \|v - \mathcal{P}_h^n v\|_{L^2(\Omega_\eta^n)}^2 &\leq \|v - \mathcal{P}_h^n v\|_{\Omega_\eta^n} \|\tilde{z} - \tilde{z}_h\|_{\Omega_\eta^n} + \left| \sum_{E \in \mathcal{E}_{h,B}^n} h \int_E \llbracket \partial_{\mathbf{n}}(\tilde{v} - \mathcal{P}_h^n \tilde{v}) \rrbracket \llbracket \partial_{\mathbf{n}}(\tilde{z} - \tilde{z}_h) \rrbracket \right| \\ &\lesssim h^5 |\tilde{v}|_{H^5(D)} \|v - \mathcal{P}_h^n v\|_{L^2(\Omega_\eta^n)}. \end{aligned}$$

This finishes the proof. \square

5.2. The stability. Now we are ready to prove the stability of numerical solutions.

THEOREM 5.2. *Suppose Assumptions 3.3 and 4.1 hold and that the penalty parameter γ_0 is large enough in \mathcal{A}_h^n . Assume $\gamma_0\tau \leq 1$ and $h = O(\tau)$. Then for $4 \leq m \leq N$,*

$$\|u_h^m\|_{L^2(\Omega_\eta^n)}^2 + \sum_{n=4}^m \tau \|u_h^n\|_{\mathcal{T}_h^n}^2 \lesssim \sum_{n=4}^m \tau \|f^n\|_{L^2(\Omega_\eta^n)}^2 + \sum_{i=0}^3 \left(\|u_h^i\|_{L^2(\Omega_\eta^i)}^2 + \tau \|u_h^i\|_{H^1(\Omega_\eta^i)}^2 \right). \quad (5.13)$$

Proof. Write $\tilde{U}_h^{n-i,n} = \mathcal{P}_h^n(U_h^{n-i,n}) \in V_h^n$ for convenience. We choose $v_h = 2u_h^n - \tilde{U}_h^{n-1,n}$ as a test function in (4.7). The telescope formula of BDF-4 (see [18]) shows that

$$\sum_{i=1}^5 \|\Psi_i^n\|_{L^2(\Omega_\eta^n)}^2 - \sum_{i=1}^4 \|\Phi_i^n\|_{L^2(\Omega_\eta^n)}^2 + \tau \mathcal{A}_h^n(u_h^n, 2u_h^n - \tilde{U}_h^{n-1,n}) = A_1^n + A_2^n, \quad (5.14)$$

where $A_1^n = \tau(f^n, 2u_h^n - \tilde{U}_h^{n-1,n})_{\Omega_\eta^n}$, $A_2^n = \sum_{i=0}^4 \lambda_i(U_h^{n-i,n}, \tilde{U}_h^{n-1,n} - U_h^{n-1,n})_{\Omega_\eta^n}$, and

$$\Psi_i^n = \sum_{j=1}^i c_{i,j} U_h^{n+1-j,n}, \quad \Phi_i^n = \sum_{j=1}^i c_{i,j} U_h^{n-j,n} = \Psi_i^{n-1} \circ \mathbf{X}_\tau^{n,n-1}.$$

The coefficients $c_{i,j}$ are real and given in [18, Table 2.2]. We extend the discrete solutions to D according to (4.2) such that $u_h^n \in V_h$. By Lemma A.3, Φ_i^n can be estimated as follows

$$\|\Phi_i^n\|_{L^2(\Omega_\eta^n)}^2 \leq (1 + C\tau) \|\Psi_i^{n-1}\|_{L^2(\Omega_\eta^{n-1})}^2 + C\tau \sum_{j=1}^i \|u_h^{n-j}\|_{L^2(\Omega_\eta^{n-j})}^2. \quad (5.15)$$

Next we summarize from Lemmas A.1 and A.2 that, for $\mu = 0, 1$,

$$\|U_h^{n-j,n}\|_{L^2(\Gamma_\eta^n)}^2 \leq (1 + C\tau) \|u_h^{n-j}\|_{L^2(\Gamma_\eta^{n-j})}^2 + C\tau^6 h^{-2} \|u_h^{n-j}\|_{H^1(\Omega_\eta^{n-j})}^2, \quad (5.16)$$

$$\|U_h^{n-j,n}\|_{H^1(\Gamma_\eta^n)}^2 \lesssim h^{-1} \|u_h^{n-j}\|_{H^1(\Omega_\eta^{n-j})}^2, \quad (5.17)$$

$$\|\nabla^\mu U_h^{n-j,n}\|_{L^2(\Omega_\eta^n)}^2 \leq (1 + C\tau) \|\nabla^\mu u_h^{n-j}\|_{L^2(\Omega_\eta^{n-j})}^2 + C\tau^6 h^{-1} \|\nabla^\mu u_h^{n-j}\|_{L^2(\Omega_\eta^{n-j})}^2. \quad (5.18)$$

Inserting (5.16)–(5.18) into (4.9) yields $\|\|U_h^{n-j,n}\|\|_{\Omega_\eta^n} \lesssim \|\|u_h^{n-j}\|\|_{\mathcal{T}_h^{n-j}}$. Remember that $\gamma_0\tau \leq 1$ and $h = O(\tau)$. Using the definition of \mathcal{P}_h^n and the Cauchy-Schwarz inequality, we have

$$\begin{aligned} \mathcal{A}_h^n(u_h^n, 2u_h^n - \tilde{U}_h^{n-1,n}) &= 2\mathcal{A}_h^n(u_h^n, u_h^n) - a_h^n(u_h^n, U_h^{n-1,n}) \\ &\geq \frac{3}{2} \|\|u_h^n\|\|_{\mathcal{T}_h^n}^2 - \frac{3\gamma_0}{5h} \|u_h^n\|_{L^2(\Gamma_\eta^n)}^2 - C\gamma_0^{-1} \|u_h^n\|_{H^1(\Omega_\eta^n)}^2 - \frac{1}{2} \|U_h^{n-1,n}\|_{H^1(\Omega_\eta^n)}^2 \\ &\quad - C\gamma_0^{-1} \|u_h^{n-1}\|_{H^1(\Omega_\eta^{n-1})}^2 - \frac{3\gamma_0}{5h} \|U_h^{n-1,n}\|_{L^2(\Gamma_\eta^n)}^2 \\ &\geq (0.9 - C\gamma_0^{-1}) \|\|u_h^n\|\|_{\mathcal{T}_h^n}^2 - (0.6 + C\gamma_0^{-1}) \|\|u_h^{n-1}\|\|_{\mathcal{T}_h^{n-1}}^2. \end{aligned} \quad (5.19)$$

By (5.5) and $\|U_h^{n-1,n}\|_{\Omega_\eta^n} \lesssim \|u_h^{n-1}\|_{\mathcal{T}_h^{n-1}}$, the right hand side of (5.14) satisfies

$$A_1^n \leq 2\tau \|f^n\|_{L^2(\Omega_\eta^n)}^2 + \tau \|u_h^n\|_{L^2(\Omega_\eta^n)}^2 + 2\tau \|U_h^{n-1,n}\|_{L^2(\Omega_\eta^n)}^2 + C\tau^3 \|U_h^{n-1,n}\|_{\Omega_\eta^n}^2, \quad (5.20)$$

$$A_2^n \leq C\tau \sum_{j=0}^4 \|U_h^{n-j,n}\|_{L^2(\Omega_\eta^n)}^2 + \frac{\tau}{10} \|u_h^{n-1}\|_{\mathcal{T}_h^{n-1}}^2. \quad (5.21)$$

Substituting (5.15) and (5.19)–(5.21) into (5.14), we can find two positive constants C_0 and C_1 which are independent of η , τ , and h , such that

$$\begin{aligned} & \sum_{i=1}^4 \left[\|\Psi_i^n\|_{L^2(\Omega_\eta^n)}^2 - \|\Psi_i^{n-1}\|_{L^2(\Omega_\eta^{n-1})}^2 \right] + 0.9\tau \|u_h^n\|_{\mathcal{T}_h^n}^2 - 0.7\tau \|u_h^{n-1}\|_{\mathcal{T}_h^{n-1}}^2 \\ & \leq C_0\tau \sum_{j=0}^4 \|u_h^{n-j}\|_{L^2(\Omega_\eta^{n-j})}^2 + C_1\gamma_0^{-1}\tau \sum_{j=0}^4 \|u_h^{n-j}\|_{\mathcal{T}_h^{n-j}}^2 + 2\tau \|f^n\|_{L^2(\Omega_\eta^n)}^2. \end{aligned} \quad (5.22)$$

Taking the sum of (5.22) over $4 \leq n \leq m$ and letting $5C_1\gamma_0^{-1} \leq 0.1$, we obtain

$$\sum_{i=1}^4 \|\Psi_i^m\|_{L^2(\Omega_\eta^m)}^2 + \tau \sum_{n=4}^m \|u_h^n\|_{\mathcal{T}_h^n}^2 \lesssim \sum_{j=0}^3 \tau \|u_h^j\|_{\mathcal{T}_h^j}^2 + \sum_{n=0}^m \tau \left(\|u_h^n\|_{L^2(\Omega_\eta^n)}^2 + \|f^n\|_{L^2(\Omega_\eta^n)}^2 \right). \quad (5.23)$$

Since $\Psi_1^m = 0.06u_h^m$ by [18, Table 2.2], the proof is finished by using Gronwall's inequality. \square

6. A priori error estimates. The purpose of this section is to establish the a priori error estimates for finite element solutions.

6.1. Extended solution. Since $\Omega_\eta^n \setminus \Omega_{t_n} \neq \emptyset$ in general, we follow Lehrenfeld and Olshanskii [14] to extend the exact solution u to the exterior of Ω_t . For convenience, we define $Q_T = \{(\mathbf{x}, t) : \mathbf{x} \in \Omega_t, t \in [0, T]\}$ and

$$L^\infty(0, T; H^m(\Omega_t)) = \left\{ v \in L^2(Q_T) : \operatorname{esssup}_{t \in [0, T]} \|v(\mathbf{X}(t; 0, \cdot), t)\|_{H^m(\Omega_0)} < +\infty \right\}, \quad m \geq 0.$$

By [23, Chapter 6], there is an extension operator $\mathbf{E}_0: H^5(\Omega_0) \rightarrow H^5(\mathbb{R}^2)$ such that

$$(\mathbf{E}_0 w)|_{\Omega_0} = w, \quad \|\mathbf{E}_0 w\|_{H^5(\mathbb{R}^2)} \lesssim \|w\|_{H^5(\Omega_0)}, \quad \forall w \in H^5(\Omega_0).$$

Since $\mathbf{X}(t; 0, \cdot)$ is one-to-one, its inverse is denoted by $\mathbf{X}(0; t, \cdot)$. Then $\Omega_0 = \mathbf{X}(0; t, \Omega_t)$. We can define an extension operator from $H^5(\Omega_t)$ to $H^5(\mathbb{R}^2)$ as

$$\mathbf{E}_t w := [\mathbf{E}_0(w \circ \mathbf{X}(t; 0, \cdot))] \circ \mathbf{X}(0; t, \cdot).$$

The global extension operator $\mathbf{E}: L^\infty(0, T; H^5(\Omega_t)) \rightarrow L^\infty(0, T; H^5(\mathbb{R}^2))$ is defined as

$$(\mathbf{E}v)(t) = \mathbf{E}_t(v(t)) \quad \forall t \in [0, T].$$

By (3.6) and arguments similar to [14], we have the stability estimates for the extension operator

$$\begin{cases} \|\mathbf{E}v\|_{H^5(\mathbb{R}^2 \times [0, T])} \leq C\|v\|_{H^5(Q_T)}, \\ \|\mathbf{E}v(t)\|_{H^m(\mathbb{R}^2)} \leq C\|v(t)\|_{H^m(\Omega_t)}, \quad 1 \leq m \leq 5, \\ \|\partial_t(\mathbf{E}v)(t)\|_{H^1(\mathbb{R}^2)} \leq C[\|v(t)\|_{H^2(\Omega_t)} + \|(\partial_t v)(t)\|_{H^1(\Omega_t)}], \end{cases} \quad (6.1)$$

where the constant $C > 0$ depends only on Ω_0 and $\|\mathbf{w}\|_{C^4(\mathbb{R}^2 \times [0, T])}$.

Let u be the exact solution to (2.1) and define $\tilde{u} = \mathbf{E}u$, $u^n := \tilde{u}(t_n)$, and $U^{m,n} := u^m \circ \mathbf{X}^{n,m}$. Multiplying $\sum_{i=0}^4 \lambda_i U^{n-i,n} - \tau \Delta u^n$ with $v_h \in V_h^n$ and using integration by parts, we have

$$\frac{1}{\tau} \sum_{i=0}^4 \lambda_i (U^{n-i,n}, v_h)_{\Omega_\eta^n} + a_h^n(u^n, v_h) = \int_{\Gamma_\eta^n} u^n \left(\frac{\gamma_0}{h} v_h - \partial_n v_h \right) + (\tilde{f}^n + R^n, v_h)_{\Omega_\eta^n}, \quad (6.2)$$

where $\tilde{f}^n = \frac{\partial \tilde{u}}{\partial t}(t_n) + \mathbf{w}(t_n) \cdot \nabla u^n - \Delta u^n$ and $R^n = \tau^{-1} \sum_{i=0}^4 \lambda_i U^{n-i,n} - \frac{\partial \tilde{u}}{\partial t}(t_n) - \mathbf{w}(t_n) \cdot \nabla u^n$.

6.2. Error estimates. Now we present the main theorem of this section. Suppose that the exact solution u and the source function f satisfy

$$M_u := \|u\|_{H^5(Q_T)}^2 + \|u\|_{L^\infty(0, T; H^5(\Omega_t))}^2 + \|\partial_t u\|_{L^\infty(0, T; H^1(\Omega_t))}^2 + \|f\|_{L^\infty(0, T; H^1(D))}^2 < \infty,$$

and that the pre-calculated initial values satisfy

$$\|u^i - u_h^i\|_{L^2(\Omega_h^i)}^2 + \tau \| \|u^i - u_h^i\|_{\mathcal{T}_h^i}^2 \leq C_0 \tau^8, \quad 0 \leq i \leq 3. \quad (6.3)$$

THEOREM 6.1. *Suppose the assumptions in Theorem 5.2 hold. Then for any $4 \leq m \leq N$,*

$$\|u^m - u_h^m\|_{L^2(\Omega_\eta^m)}^2 + \sum_{n=4}^m \tau \| \|u^n - u_h^n\|_{\mathcal{T}_h^n}^2 \lesssim (C_0 + M_u) \tau^8.$$

Proof. Write $\rho^n := u^n - \mathcal{P}_h^n u^n$ and $\theta_h^n := \mathcal{P}_h^n u^n - u_h^n$. By Lemma 5.1, (5.4), and (6.1), we have

$$\max_{1 \leq n \leq N} \|\rho^n\|_{L^2(\Omega_\eta^n)}^2 + \sum_{n=1}^N \tau \| \|\rho^n\|_{\mathcal{T}_h^n}^2 \lesssim \tau^8 \|u\|_{L^\infty(0, T; H^5(\Omega_t))}^2. \quad (6.4)$$

It is left to estimate θ_h^n for $4 \leq n \leq N$. The arguments are similar to the proof of Theorem 5.2. Due to (6.3)–(6.4) and (4.8), the pre-calculated initial values satisfy

$$\|\theta_h^i\|_{L^2(\Omega_h^i)}^2 + \tau \| \|\theta_h^i\|_{\mathcal{T}_h^i}^2 \lesssim \|\theta_h^i\|_{L^2(\Omega_\eta^i)}^2 + \tau \| \|\theta_h^i\|_{\mathcal{T}_h^i}^2 \lesssim C_0 \tau^8, \quad 0 \leq i \leq 3. \quad (6.5)$$

Define $\Theta_h^{m,n} = \theta_h^m \circ \mathbf{X}_\tau^{n,m}$ and $\zeta^{m,n} = (u^m \circ \mathbf{X}_\tau^{n,m} - u^m \circ \mathbf{X}^{n,m}) - \rho^m \circ \mathbf{X}_\tau^{n,m}$. Subtracting (4.7) from (6.2) and using (5.2), we get

$$\sum_{i=0}^4 \lambda_i (\theta_h^{n-i,n}, v_h)_{\Omega_\eta^n} + \tau \mathcal{A}_h^n(\theta_h^n, v_h) = \tau (g^n, v_h)_{\Omega_\eta^n} + \tau \ell_n(v_h), \quad (6.6)$$

where $g^n = R^n + \tau^{-1} \sum_{i=0}^4 \lambda_i \zeta^{n-i,n}$ and $\ell_n(v_h) = (\tilde{f}^n - f^n, v_h)_{\Omega_\eta^n} + \int_{\Gamma_\eta^n} (\gamma_0 h^{-1} v_h - \partial_n v_h) u^n$.

Choosing $v_h^n = 2\theta_h^n - \mathcal{P}_h^n \Theta_h^{n-1,n}$ in (6.6) and using (5.13) and (6.3), we obtain

$$\|\theta_h^m\|_{L^2(\Omega_\eta^m)}^2 + \tau \sum_{n=4}^m \| \|\theta_h^n\|_{\mathcal{T}_h^n}^2 \lesssim C_0 \tau^8 + \sum_{n=4}^m \tau \left[\|g^n\|_{L^2(\Omega_\eta^n)}^2 + |\ell_n(v_h^n)| \right]. \quad (6.7)$$

It suffices to estimate g^n and $\ell_n(v_h^n)$ on the right-hand side of (6.7).

Applying Taylor's formula to R^n yields

$$\|R^n\|_{L^2(\Omega_\eta^n)}^2 = \int_{\Omega_\eta^n} \left| \sum_{i=1}^4 \frac{\lambda_i}{4! \tau} \int_{t_{n-i}}^{t_n} (t_n - t)^4 \frac{d^5}{dt^5} u(\mathbf{X}(t; t_n, \mathbf{x}), t) dt \right|^2 d\mathbf{x} \lesssim \tau^7 \|u\|_{H^5(D \times (t_{n-4}, t_n))}^2.$$

Let $\mathcal{I}_h u^{n-i} \in V_h$ be the Scott-Zhang interpolation of u^{n-i} and define $\rho_h^{n-i} = \mathcal{I}_h u^{n-i} - \mathcal{P}_h^{n-i} u^{n-i}$. From (6.4), we obtain

$$\|\rho_h^{n-i}\|_{L^2(\Omega_h^{n-i})} \leq \|\rho^{n-i}\|_{L^2(\Omega_h^{n-i})} + \|u^{n-i} - \mathcal{I}_h u^{n-i}\|_{L^2(\Omega_h^{n-i})} \lesssim h^5 \|u^{n-i}\|_{H^5(D)}.$$

Moreover, combining Lemma A.2 and Lemma 4.2 shows

$$\begin{aligned} \|\rho_h^{n-i} \circ \mathbf{X}_\tau^{n, n-i}\|_{L^2(\Omega_\eta^n)} &\lesssim \|u^{n-i} - \mathcal{I}_h u^{n-i}\|_{L^2(\Omega_h^{n-i})} + \|\rho_h^{n-i} \circ \mathbf{X}_\tau^{n, n-i}\|_{L^2(\Omega_\eta^n)} \\ &\lesssim h^5 \|u^{n-i}\|_{H^5(D)} + \|\rho_h^{n-i}\|_{L^2(\Omega_\eta^{n-i})} + \tau^{2.5} \|\rho_h^{n-i}\|_{L^2(\Omega_h^{n-i})} \\ &\lesssim \tau^5 \|u^{n-i}\|_{H^5(D)}. \end{aligned}$$

Using (3.7) and Lemma A.1, we get $\|\zeta^{n-i, n}\|_{L^2(\Omega_\eta^n)} \lesssim \tau^5 \|u^{n-i}\|_{H^5(D)}$; and from (6.1), we have

$$\sum_{n=4}^m \tau \|g^n\|_{L^2(\Omega_\eta^n)}^2 \lesssim \tau^8 (\|u\|_{L^\infty(0, T; H^5(\Omega_t))}^2 + \|u\|_{H^5(Q_T)}^2). \quad (6.8)$$

Next we estimate $\ell_n(v_h^n)$. Using Lemma A.4 and the identity $\tilde{f}^n = f^n$ in Ω_{t_n} , we find that

$$|(\tilde{f}^n - f^n, v_h^n)_{\Omega_\eta^n}| = |(\tilde{f}^n - f^n, v_h^n)_{\Omega_\eta^n \setminus \Omega_{t_n}}| \lesssim \tau^{4.5} \|\tilde{f}^n - f^n\|_{H^1(\Omega_\eta^n)} \|v_h^n\|_{L^2(\Omega_\eta^n)}. \quad (6.9)$$

Since $u^n = 0$ on Γ_{t_n} , Taylor's formula and Lemma 3.4 indicate

$$\|u^n\|_{L^2(\Gamma_\eta^n)}^2 = \int_0^{L_0} (u^n \circ \chi_n - u^n \circ \hat{\chi}_n)^2 |\chi_n'| \lesssim \tau^{10} \|u^n\|_{H^1(D)}^2.$$

Using inverse estimate, we obtain

$$|\ell_n(v_h^n)| \lesssim \tau^{4.5} \|\tilde{f}^n - f^n\|_{H^1(\Omega_\eta^n)} \|v_h^n\|_{L^2(\Omega_\eta^n)} + \tau^4 \|u^n\|_{H^1(D)} \|v_h^n\|_{L^2(\Gamma_\eta^n)}. \quad (6.10)$$

The techniques for estimating $v_h^n = 2\theta_h^n - \mathcal{P}_h^n \Theta_h^{n-1, n}$ are similar to (5.20). They use Lemma 4.2, (5.3), (5.6), Lemma A.1, and Lemma A.2. We omit the details and just present the results

$$\begin{aligned} \|v_h^n\|_{L^2(\Omega_h^n)}^2 &\lesssim \|\theta_h^n\|_{L^2(\Omega_\eta^n)}^2 + \|\theta_h^{n-1}\|_{L^2(\Omega_\eta^{n-1})}^2 + h^2 \|\|\theta_h^n\|\|_{\mathcal{T}_h^n}^2 + h^2 \|\|\theta_h^{n-1}\|\|_{\mathcal{T}_h^{n-1}}^2, \\ \|v_h^n\|_{L^2(\Gamma_\eta^n)}^2 &\lesssim h \mathcal{J}_0^n(\theta_h^n, \theta_h^n) + h \|\|\Theta_h^{n-1, n}\|\|_{\Omega_\eta^n}^2 \lesssim h \|\|\theta_h^n\|\|_{\mathcal{T}_h^n}^2 + h \|\|\theta_h^{n-1}\|\|_{\mathcal{T}_h^{n-1}}^2. \end{aligned}$$

Inserting the estimates into (6.9) and (6.10) yields

$$\sum_{n=4}^m \tau |\ell_n(v_h^n)| \lesssim \tau^8 M_u + \tau^2 \sum_{n=3}^m \left(\|\|\theta_h^n\|\|_{L^2(\Omega_\eta^n)}^2 + \|\|\theta_h^n\|\|_{\mathcal{T}_h^n}^2 \right). \quad (6.11)$$

Finally, we insert (6.8)–(6.11) into (6.7) and let τ be small enough. This yields

$$\|\|\theta_h^m\|\|_{L^2(\Omega_\eta^m)}^2 + \tau \sum_{n=4}^m \|\|\theta_h^n\|\|_{\mathcal{T}_h^n}^2 \lesssim (C_0 + M_u) \tau^8. \quad (6.12)$$

The proof is finished by combining (6.4) and (6.12). \square

7. Numerical experiments. Now we use two numerical experiments to verify the convergence order of the UCFEM. The exact solution is set by $u(\mathbf{x}, t) = e^{-t} \sin(\pi x_1) \sin(\pi x_2)$. To simplify the computation, we set the pre-calculated initial values by the exact solution, namely, $u_h^j = u(t_j)$, for $0 \leq j \leq 3$. Throughout the section, we set $\gamma_0 = 800$, $\gamma_1 = 1/\gamma_0$, and $\eta \leq 0.5\tau$. The approximation error is measured with the quantity $e^N = [\|u(\cdot, T) - u_h^N\|_{L^2(\Omega_\eta^N)}^2 + \sum_{n=4}^N \tau |u - u_h^n|_{H^1(\Omega_\eta^n)}^2]^{1/2}$.

7.1. A rotating elliptic ring. This example is to test the robustness and optimal convergence of the UCFEM for rigid motions. The velocity is set by $\mathbf{w} = (0.5 - x_2, x_1 - 0.5)^\top$. The initial domain Ω_0 is an elliptical ring centered at $(0.5, 0.5)$. The inner boundary is an ellipse with major axis equal to 0.22 and minor axis equal to 0.1. The outer boundary is an ellipse with major axis equal to 0.3 and minor axis equal to 0.15. The ring has rotated half a circle counterclockwise at $T = \pi$.

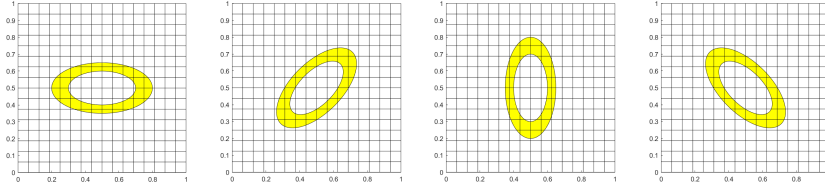


Fig. 7.1: The approximate domains at $t_n = 0, \pi/4, \pi/2$, and $3\pi/4$, respectively ($h = 2^{-4}$).

Table 7.1: Convergence orders for Example 1 ($h = \tau/\pi$).

h	e^N	order	h	e^N	order
2^{-4}	2.98e-06	—	2^{-6}	1.67e-08	3.86
2^{-5}	2.43e-07	3.62	2^{-7}	1.09e-09	3.93

Since the rigid motion of the ring is an isometry, in Algorithm 3.1 there is no need to redistribute the markers on the boundary. The interface tracking error only comes from cubic spline interpolations. Our method can achieve good accuracy even on coarse meshes. Table 7.1 shows that the optimal convergence $e^N \sim \tau^4$ is obtained asymptotically.

7.2. Vortex flow. The second example is to test the robustness and optimal convergence of the UCFEM for severely deformed domains. The initial domain Ω_0 is the disk whose radius is 0.15 and center is $(0.5, 0.75)$. The driving velocity is set by

$$\mathbf{w} = \cos(\pi t/4) (\sin^2(\pi x_1) \sin(2\pi x_2), -\sin^2(\pi x_2) \sin(2\pi x_1))^\top.$$

At time $T = 2$, Ω_T is stretched into a snake-like domain (see Fig. 7.2). In this example, Γ_t suffers a large deformation and yields a local C^1 -discontinuity at the final time. To guarantee the high accuracy of the method, we use Algorithm 3.1 to track the boundary and adjust the set of markers dynamically in time. Since the exact solution is analytic, we can still observe optimal convergence as shown in Tables 7.2.

Table 7.2: Convergence orders for Example 2 ($h = \tau$).

h	e^N	order	h	e^N	order
2^{-4}	2.43e-06	—	2^{-6}	4.56e-09	4.44
2^{-5}	9.90e-08	4.62	2^{-7}	2.34e-10	4.29

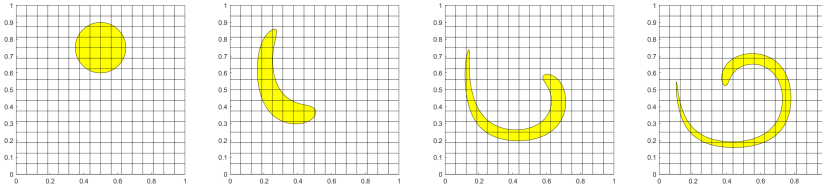


Fig. 7.2: The approximate domains Ω_η^n at $t_n = 0, 1/2, 1,$ and $2,$ respectively ($h = 2^{-4}$).

REFERENCES

- [1] E. BURMAN AND P. HANSBO, *Fictitious domain finite element methods using cut elements: I. A stabilized Lagrange multiplier method*, Comput. Methods Appl. Mech. Engrg., 199 (2010), pp. 2680–2686.
- [2] E. BURMAN, S. CLAUS, P. HANSBO, M. G. LARSON, AND A. MASSING, *CutFEM: Discretizing geometry and partial differential equations*, Internat. J. Numer. Methods Engrg., 104 (2015), pp. 472–501.
- [3] A. J. CHORIN AND J. E. MARSDEN, *A mathematical introduction to fluid mechanics*, Springer-Verlag, New York, 1990.
- [4] J. DOLBOW, N. MOËS, AND T. BELYTSCHKO, *An extended finite element method for modeling crack growth with frictional contact*, Comput. Methods Appl. Mech. Engrg., 190 (2001), pp. 6825–6846.
- [5] S. FREI AND T. RICHTER, *A second order time-stepping scheme for parabolic interface problems with moving interfaces*, ESAIM Math. Model. Numer. Anal., 51 (2017), pp. 1539–1560.
- [6] T. P. FRIES AND A. ZILIAN, *On time integration in the XFEM*, Internat. J. Numer. Methods Engrg., 79 (2009), pp. 69–93.
- [7] S. GROSS AND A. REUSKEN, *Numerical Methods for Two-Phase Incompressible Flows*, Springer-Verlag, Berlin, 2011.
- [8] R. GUO, *Solving parabolic moving interface problems with dynamical immersed spaces on unfitted meshes: fully discrete analysis*, SIAM J. Numer. Anal., 59 (2021), pp. 797–828.
- [9] J. GUZMÁN AND M. OLSHANSKII, *Inf-sup stability of geometrically unfitted Stokes finite elements*, Math. Comp., 87 (2018), pp. 2091–2112.
- [10] A. HANSBO AND P. HANSBO, *An unfitted finite element method, based on Nitsche’s method, for elliptic interface problems*, Comput. Methods Appl. Mech. Engrg., 191 (2002), pp. 5537–5552.
- [11] J. HASLINGER AND Y. RENARD, *A new fictitious domain approach inspired by the extended finite element method*, SIAM J. Numer. Anal., 47 (2009), pp. 1474–1499.
- [12] C. LEHRENFELD, *The nitsche XFEM-DG space-time method and its implementation in three space dimensions*, SIAM J. Sci. Comput., 37 (2015), pp. A245–A270.
- [13] C. LEHRENFELD AND A. REUSKEN, *Analysis of a Nitsche XFEM-DG discretization for a class of two-phase mass transport problems*, SIAM J. Numer. Anal., 51 (2013), pp. 958–983.
- [14] C. LEHRENFELD AND M. OLSHANSKII, *An Eulerian finite element method for PDEs in time-dependent domains*, ESAIM Math. Model. Numer. Anal., 53 (2019), pp. 585–614.
- [15] R. J. LEVEQUE AND Z. LI, *The immersed interface method for elliptic equations with discontinuous coefficients and singular sources*, SIAM J. Numer. Anal., 31 (1994), pp. 1019–1044.
- [16] Z. LI AND K. ITO, *The Immersed Interface Method*, Society for Industrial and Applied Mathematics, 2006.
- [17] T. LIN, Y. LIN AND X. ZHANG, *Partially penalized immersed finite element methods for elliptic interface problems*, SIAM J. Numer. Anal., 53 (2015), pp. 1121–1144.
- [18] J. LIU, *Simple and efficient ALE methods with provable temporal accuracy up to fifth order for the Stokes equations on time-varying domains*, SIAM J. Numer. Anal., 51 (2013), pp. 743–772.
- [19] Y. LOU AND C. LEHRENFELD, *Isoparametric unfitted BDF-Finite element method for PDEs on evolving domains*, arXiv:2105.09162v1.
- [20] A. MASSING, M. G. LARSON, A. LOGG, AND M. E. ROGNES, *A stabilized Nitsche fictitious domain method for the Stokes problem*, J. Sci. Comput., 61 (2014), pp. 604–628.
- [21] S. NICAISE AND S. A. SAUTER, *Efficient numerical solution of Neumann problems on complicated domains*, Calcolo, 43 (2006), pp. 95–120.
- [22] L.R. SCOTT AND S. ZHANG, *Finite element interpolation of nonsmooth functions satisfying boundary conditions*, Math. Comp., 54 (1990), pp. 483–493.
- [23] E.M. STEIN, *Singular Integrals and Differentiability Properties of Functions*, Princeton University Press, Princeton, New Jersey, 1970.

- [24] J.H. VERNVER, *Explicit Runge-Kutta methods with estimates of the local truncation error*, SIAM J. Numer. Anal., 15 (1978), pp. 708–759.
- [25] H. WU AND Y. XIAO, *An unfitted hp-interface penalty finite element method for elliptic interface problems*, J. Comp. Math., 37 (2019), pp. 316–339.
- [26] Q. ZHANG AND A. FOGELSON, *Fourth-and higher-order interface tracking via mapping and adjusting regular semianalytic sets represented by cubic splines*, SIAM J. Sci. Comput., 40 (2018), pp. A3755–A3788.

Appendix A. Estimates of $v \circ \mathbf{X}_\tau^{n,n-i}$ and $v \circ \mathbf{X}_\tau^{n,n-i}$. In this appendix, we prove some useful estimates for $v \circ \mathbf{X}_\tau^{n,n-i}$ and $v \circ \mathbf{X}_\tau^{n,n-i}$ with $0 \leq i \leq 4$.

LEMMA A.1. *Suppose $h = O(\tau) = O(\eta^{4/5})$ and $\Omega \cup \mathbf{X}_\tau^{n,n-i}(\Omega) \cup \mathbf{X}^{n,n-i}(\Omega) \subset D$. There exists an $h_0 > 0$ such that, for any $h \in (0, h_0]$, $v \in H^1(D)$, and $v_h \in V_h$,*

$$\|\nabla^\mu(v \circ \mathbf{X}_\tau^{n,n-i})\|_{L^2(\Omega)}^2 \leq (1 + C\tau) \|\nabla^\mu v\|_{L^2(\mathbf{X}_\tau^{n,n-i}(\Omega))}^2, \quad \mu = 0, 1, \quad (\text{A.1})$$

$$\|v \circ \mathbf{X}_\tau^{n,n-i} - v \circ \mathbf{X}_\tau^{n,n-i}\|_{L^2(\Omega)} \lesssim \tau^6 |v|_{H^1(D)}, \quad (\text{A.2})$$

$$|v_h \circ \mathbf{X}_\tau^{n,n-i}|_{H^1(\Gamma_\eta^n)}^2 \lesssim h^{-1} |v_h|_{H^1(\Omega_h^{n-i})}^2, \quad (\text{A.3})$$

$$\|v_h \circ \mathbf{X}_\tau^{n,n-i}\|_{L^2(\Gamma_\eta^n)}^2 \leq (1 + C\tau) \|v_h\|_{L^2(\Gamma_\eta^{n-i})}^2 + C\tau^4 \|v_h\|_{H^1(\Omega_h^{n-i})}^2. \quad (\text{A.4})$$

Proof. Inequality (A.1) is obtained directly by changing variables of integration and using (3.6). Inequality (A.2) is a direct consequence of (3.7). Moreover, (A.3) can be proven easily by using scaling arguments, norm equivalence, and the results in (3.6).

To prove (A.4), we note that

$$\|v_h \circ \mathbf{X}_\tau^{n,n-i}\|_{L^2(\Gamma_\eta^n)}^2 = \int_0^{L_0} |v_h \circ \chi_{n-i}|^2 |\chi'_n| + \int_0^{L_0} (|v_h \circ \mathbf{X}_\tau^{n,n-i} \circ \chi_n|^2 - |v_h \circ \chi_{n-i}|^2) |\chi'_n|.$$

Remember from (4.1) that $\min_{\mathbf{x} \in \partial\Omega_h^m} \text{dist}(\mathbf{x}, \Gamma_\eta^m) \geq h/2$ for any $m > 0$. Then, for h small enough,

$$\mathbf{X}_\tau^{n,n-i}(\Omega_\eta^n) \subset \Omega_h^{n-i}, \quad \mathbf{X}_\tau^{n-i,n}(\Omega_\eta^{n-i}) \subset \Omega_h^n. \quad (\text{A.5})$$

By Theorem 3.5 and the relation $\eta = O(\tau^{5/4})$, it is easy to see that

$$\begin{cases} \|\chi_n - \mathbf{X}_\tau^{n-i,n} \circ \chi_{n-i}\|_{C([0, L_0])} \lesssim \tau^6, \\ \|\mathbf{X}_\tau^{n,n-i} \circ \chi_n - \chi_{n-i}\|_{C([0, L_0])} \lesssim \|\chi_n - \mathbf{X}_\tau^{n-i,n} \circ \chi_{n-i}\|_{C([0, L_0])} \lesssim \tau^6. \end{cases} \quad (\text{A.6})$$

With (3.6), it is standard to derive $|\chi'_{n-i}| \leq |\chi'_n| + C\tau$ and $|\chi'_n| |\chi'_{n-i}|^{-1} \leq 1 + C\tau$. So we have

$$\int_0^{L_0} |v_h \circ \chi_{n-i}|^2 |\chi'_n| \leq (1 + C\tau) \int_0^{L_0} |v_h \circ \chi_{n-i}|^2 |\chi'_{n-i}| = (1 + C\tau) \|v_h\|_{L^2(\Gamma_\eta^{n-i})}^2. \quad (\text{A.7})$$

Using Taylor's formula, inequality (A.6), and norm equivalence on each element, we also have

$$\int_0^{L_0} (|v_h \circ \mathbf{X}_\tau^{n,n-i} \circ \chi_n|^2 - |v_h \circ \chi_{n-i}|^2) |\chi'_n| \lesssim \tau^6 h^{-2} \|v_h\|_{H^1(\Omega_h^{n-i})}^2. \quad (\text{A.8})$$

We obtain (A.4) from (A.7) and (A.8). \square

LEMMA A.2. *Suppose $h = O(\tau) = O(\eta^{4/5})$. There is a constant C independent of τ such that*

$$\|\nabla^\mu(v_h \circ \mathbf{X}_\tau^{n,n-i})\|_{L^2(\Omega_\eta^n)}^2 \leq (1 + C\tau)\|\nabla^\mu v_h\|_{L^2(\Omega_\eta^{n-i})}^2 + C\tau^5 \|\nabla^\mu v_h\|_{L^2(\Omega_h^{n-i})}^2, \quad \mu = 0, 1.$$

Proof. Clearly $\Omega_\eta^n \subset \mathbf{X}_\tau^{n-i,n}(\Omega_\eta^{n-i}) \cup D_\eta^n$ where $D_\eta^n := \Omega_\eta^n \setminus \mathbf{X}_\tau^{n-i,n}(\Omega_\eta^{n-i})$ is the narrow strip between Γ_η^n and $\mathbf{X}_\tau^{n-i,n}(\Gamma_\eta^{n-i})$. Similarly, $\mathbf{X}_\tau^{n,n-i}(D_\eta^n)$ is the narrow strip between $\mathbf{X}_\tau^{n,n-i}(\Gamma_\eta^n)$ and Γ_η^{n-i} . From (A.5) and (A.6), we have $\mathbf{X}_\tau^{n,n-i}(D_\eta^n) \subset \Omega_h^{n-i}$ and $\text{area}[K \cap \mathbf{X}_\tau^{n,n-i}(D_\eta^n)] \lesssim \tau^6 h$ for any $K \in \mathcal{T}_h$. The scaling argument shows that

$$\|v_h \circ \mathbf{X}_\tau^{n,n-i}\|_{L^2(D_\eta^n)}^2 \lesssim \sum_{K \cap \mathbf{X}_\tau^{n,n-i}(D_\eta^n) \neq \emptyset} h\tau^6 \|v_h\|_{L^\infty(K)}^2 \lesssim h^{-1}\tau^6 \|v_h\|_{L^2(\Omega_h^{n-i})}^2. \quad (\text{A.9})$$

Note that $\nabla(v_h \circ \mathbf{X}_\tau^{n,n-i}) = \mathbb{J}_\tau^{n,n-i}(\nabla v_h) \circ \mathbf{X}_\tau^{n,n-i}$. Using (A.1), we have

$$\|v_h \circ \mathbf{X}_\tau^{n,n-i}\|_{L^2(\Omega_\eta^n)}^2 \leq (1 + C\tau)\|v_h\|_{L^2(\Omega_\eta^{n-i})}^2 + h^{-1}\tau^6 \|v_h\|_{L^2(\Omega_h^{n-i})}^2.$$

The proof for the case of $\mu = 1$ is similar. \square

LEMMA A.3. *Suppose the conditions in Lemma A.2 hold. Let $w_n = \sum_{i=1}^4 v_i \circ \mathbf{X}_\tau^{n,n-i}$ and $w_{n-1} = \sum_{i=1}^4 v_i \circ \mathbf{X}_\tau^{n-1,n-i}$ with $v_i \in V_h$. There is a constant $C > 0$ independent of τ such that*

$$\|w_n\|_{L^2(\Omega_\eta^n)}^2 \leq (1 + C\tau)\|w_{n-1}\|_{L^2(\Omega_\eta^{n-1})}^2 + C\tau^5 (\|v_1\|_{L^2(D)}^2 + \cdots + \|v_4\|_{L^2(D)}^2).$$

Proof. Note that $w_n = w_{n-1} \circ \mathbf{X}_\tau^{n,n-1}$. The lemma can be proven by (A.1) and arguments similar to the proof of Lemma A.2. \square

LEMMA A.4. *Let Assumptions 2.1 and 3.3 be satisfied. Suppose $h = O(\tau) = O(\eta^{4/5})$. For any $v_h \in V_h$ and $v \in H^1(D)$,*

$$\|v_h\|_{L^2(\Omega_\eta^n \setminus \Omega_{t_n})}^2 \lesssim \tau^4 \|v_h\|_{L^2(\Omega_h^n)}^2, \quad \|v\|_{L^2(\Omega_\eta^n \setminus \Omega_{t_n})}^2 \lesssim \tau^5 \|v\|_{H^1(\Omega_\eta^n)}^2.$$

Proof. The first inequality follows from Lemma 3.4 and arguments similar to (A.9). From (3.7) and (A.6), we know that $\text{dist}(\Gamma_\eta^n, \Gamma_{t_n}) = O(\tau^5)$. The second inequality is a direct consequence of [21, Lemma 10 and (17)]. \square